RSC Advances

PAPER

View Article Online
View Journal | View Issue

Cite this: *RSC Adv.*, 2017, **7**, 14337

Cationic Salecan-based hydrogels for release of 5-fluorouracil†

Xiaoliang Qi, Junjian Li, Wei Wei, Gancheng Zuo, Ting Su, Xihao Pan, Jianfa Zhang and Wei Dong*

Salecan, a new water-soluble β-glucan, has excellent physicochemical and biological characteristics. Here, a series of pH-sensitive hydrogels based on Salecan grafted with [2-(methacryloxy)ethyl] trimethylammonium chloride were developed for controlled drug delivery. The successful preparation of the grafted hydrogels was confirmed by Fourier transform infrared spectroscopy, X-ray diffraction, and thermogravimetric analysis. After that, rheology and scanning electron microscopy tests showed that the mechanical and morphological properties of these hydrogels were strongly influenced by the Salecan content. Moreover, the swelling behavior of the resulting hydrogels was systematically studied, and the results suggested that they exhibited pH sensitivity. Loading and delivery experiments demonstrated that 5-fluorouracil was efficiently encapsulated into the hydrogel matrices and released in a predictable manner *via* pH and Salecan dose control. Finally, cell viability and adhesion assays verified the cell compatibility of the designed hydrogels. Altogether, these attributes make the Salecan-based graft hydrogel a promising platform for controlled 5-fluorouracil delivery.

Received 24th January 2017
Accepted 26th February 2017

DOI: 10.1039/c7ra01052d

rsc.li/rsc-advances

1 Introduction

Hydrogels are prepared from hydrophilic polymers with a three-dimensional (3D) network that are capable of uptaking large volumes of water without dissolving.[1–3] In particular, stimuli-responsive hydrogels, also termed intelligent hydrogels, which can undergo a reversible phase transition in response to a great deal of external stimuli including temperature,[4] light,[5] pH,[6] electric field,[7] have attracted considerable attention in medical and biological applications.[8,9] Of these intelligent hydrogel materials, the pH-responsive ones are widely investigated because the pH value is a crucial environmental factor in human bodies.[6,10,11]

In recent decades, natural polymers such as polysaccharides, have frequently been used to design intelligent hydrogel drug carriers (reserving drugs in a de-swollen state and releasing drugs in a swollen state) owing to their superior physiochemical and biological properties (*e.g.*, biodegradability, renewability and biocompatibility).[12,13] However, polysaccharide-based hydrogel drug devices have two significant inherent limitations: one is the poor mechanical strength, and the other is the lack of sustained release ability.[14] Typically, drugs are wrapped in the hydrogel matrices by simple physical forces only, resulting in a burst release of encapsulated drugs because of the relatively weak intermolecular interactions between hydrogels and drugs.[12,15] Thus, it remains a formidable challenge to design carriers that are able to release loaded drugs in a predictable fashion.[16] The fusion of natural polysaccharides and synthetic polymers may benefit to bridge these gaps and share the merits of each component.[17,18] Graft copolymerization is an effective and versatile approach to modify the architecture of native polysaccharides.[13] This technique greatly enlarges the applications of polysaccharide-constructed hydrogels.[14,19] For instance, various synthetic polymers including [2-(methacryloxy)ethyl]trimethylammonium chloride,[20] *N*-isopropylacrylamide[4] and acrylic acid,[15] have been successfully introduced into the polysaccharide skeleton. The resulting graft hydrogels has various desirable characteristics like stimuli-responsive features, moderate swelling capacity and improved mechanical strength, making them more appropriate for drug encapsulation/release.[15,19]

Salecan, a novel linear β-glucan, is produced by a new strain of *Agrobacterium* sp. *ZX09* isolated from Dongying soil by our group.[21] It is composed of α-1-3-linked and β-1-3-linked glucopyranosyl units (Fig. 1). Like other microbial polysaccharides, Salecan has fascinating biological properties including antioxidation and nontoxicity, which are typically needed in food and pharmaceutical industries.[22–24] Additionally, Salecan contains plenty of hydroxyl functional groups located on its backbone, and consequently making it convenient to be chemically modified. A series of Salecan-containing hydrogels were developed by our laboratory recently. We found that these novel gels were adequate materials to be employed in drug delivery and tissue engineering field.[16,25–27]

Center for Molecular Metabolism, Nanjing University of Science & Technology, Nanjing 210094, China. E-mail: weidong@njust.edu.cn; Fax: +86-25-84318533; Tel: +86-25-84318533

† Electronic supplementary information (ESI) available. See DOI: 10.1039/c7ra01052d

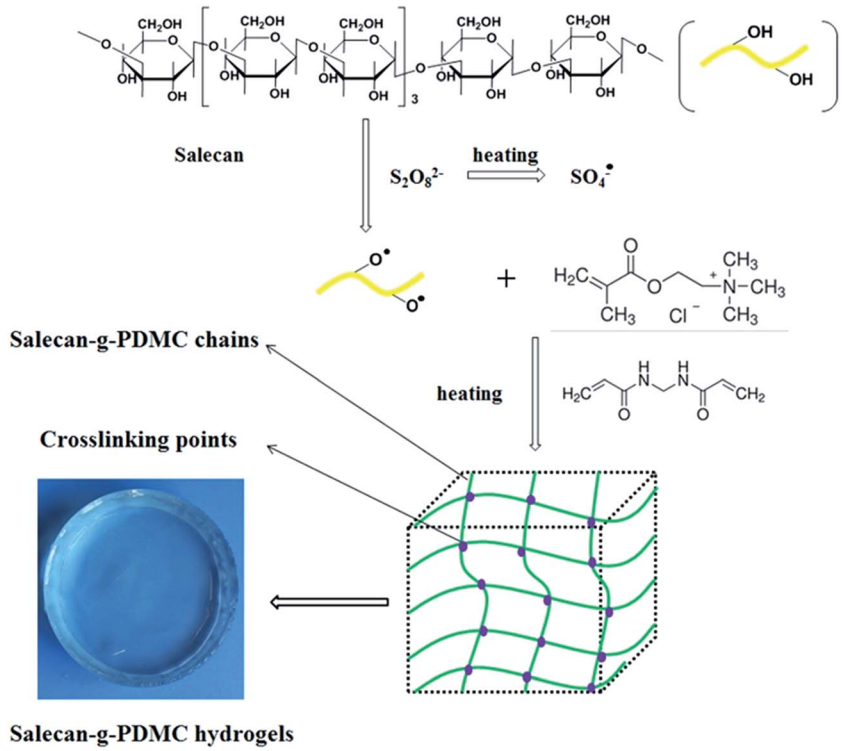

Fig. 1 Scheme showing the fabrication of Salecan-*g*-PDMC hydrogels.

[2-(Methacryloxy)ethyl]trimethylammonium chloride (DMC) is a significant monomer that is commonly used for the fabrication of functional hydrogels. By incorporation of DMC into the network, hydrogels can be used for selective removal of dyes or metal ions.[28,29] Especially, the incorporation of quaternary ammonium groups imparts hydrogels response to a number of external stimuli such as salt and pH, and thus allows their application in drug release systems.[30,31]

In the present work, we attempted to develop Salecan-*g*-PDMC hydrogels with different Salecan content for controlled release application. This is the first article, to the best of our knowledge, to design and prepare Salecan-based hydrogels for 5-fluorouracil delivery. In these novel graft hydrogels, Salecan serves as the host polymer network, and the introduction of DMC unit endows the gels with stimulus-sensitive features. We anticipate that the combination of the biocompatible characteristic of Salecan with the stimulus-sensitive property of DMC will permit efficient drug encapsulation/delivery.

2 Materials and methods

2.1. Materials

Salecan was fabricated by Nanjing University of Science & Technology. [2-(Methacryloxy)ethyl]trimethylammonium chloride (DMC, 80% in water) was provided by TCI (Shanghai, China) and applied as received. Ammonium persulfate (APS, 99.5%), 5-fluorouracil (99.0%) and *N*,*N*′-methylenebisacrylamide (MBAA, 99.0%) were acquired from Sigma-Aldrich (Shanghai, China) and used without further purification. Ethidium bromide/acridine orange (EB/AO), and bovine serum albumin (BSA) were supplied by Meilun Biotech Co., Ltd (Dalian, China). The cell proliferation and cell cytotoxicity detection kit was procured from KeyGen Biology Technology Co., Ltd (Nanjing, China).

2.2. Synthesis of Salecan-*g*-PDMC hydrogels

Hydrogels were prepared by free-radical graft copolymerization of DMC and Salecan utilizing MBAA as the cross-linking agent and APS as an initiator. Typically, variable amounts of Salecan solution (2%, w/v) were incorporated into a 50 mL three-neck flask with a magnetic stirrer, a water circulation system and a nitrogen line. Salecan solution was heated to 65 °C in a water bath and then degassed with nitrogen for 15 min to eliminate dissolved oxygen. Thereafter, a certain content of APS was added into the flask under vigorous stirring at 65 °C for 15 min to generate radicals. After cooling to 25 °C, the flask was taken out from the water bath, the DMC solution (80%, w/v) containing the calculated amount of MBAA (80 mg) was poured into the reaction system successively. The obtained precursor solution (the final volume of the mixture was fixed at 20 mL by adding deionized water) was continuously stirred at 37 °C for 10 min under nitrogen atmosphere and then introduced into a Petri dish. The dish was placed into a water bath at 60 °C 24 h. After polymerization, the formed hydrogels were gently taken out and immersed in deionized water for 4 days. During this period, the water was substituted with fresh deionized water at least two times daily so as to remove the unreacted chemicals. All gel samples were freeze-dried for further use. The feed ratios of the reaction mixtures in this work are displayed in Table 1.

Table 1 Compositions of initial reaction mixtures utilized for the fabrication of Salecan-*g*-PDMC hydrogels

	Designation				
Ingredient	PDMC	SGD1	SGD2	SGD3	SGD4
Salecan (2%, w/v) (mL)	0	2.5	5	7.5	10
DMC (80%, w/v) (mL)	1.5	1.5	1.5	1.5	1.5
MBAA (2%, w/v) (mL)	4	4	4	4	4
APS (3.2%, w/v) (mL)	1	1	1	1	1
Deionized water (mL)	13.5	11	8.5	6	3.5

2.3. Fourier transform infrared (FT-IR) spectra

FT-IR spectra were recorded by a Nicolet IS-10 spectrometer (Thermo Fisher, America) working in attenuated total reflectance mode, the resolution being 2 cm^{-1}, in the range 4000–600 cm^{-1} with a 32 scans per sample cycle.

2.4. X-ray diffraction (XRD)

XRD profiles of the samples were detected with a DMAX-2200 diffractometer (40 kV and 40 mA) equipped with a Cu Kα radiation (0.154 nm) over the range of 10–60°.

2.5. Thermogravimetric analysis (TGA)

TGA assay was conducted on a TA Q-600 thermal analyzer. The sample was heated until 600 °C at 20 °C min^{-1} in nitrogen atmosphere.

2.6. Morphology observation

The cross-section surface morphology of hydrogels was observed by a scanning electron microscope (SEM, JSM-6380LV, JEOL, Tokyo, Japan) at 30 kV. For such measurement, the prepared hydrogels were first freeze-dried and fractured in liquid nitrogen. Then, the hydrogels were pasted onto a mica sheet and vacuum coated with gold. The average pore size was evaluated from the SEM photographs by the Nano Measurer 1.2.5 software designed by Fudan University (Shanghai, China).

2.7. Mechanical properties

Mechanical performances of the developed hydrogels were studied using a Physica MCR 101 rheometer (Anton Paar) with a parallel plate of 40 mm diameter. Before the experiment, dynamic strain sweep experiments were conducted to identify the linear viscoelasticity region. Dynamic frequency sweep assays (0.01% strain) were performed on the grafted hydrogel samples in the range 0.1–10 Hz at 25 °C.

2.8. Swelling behaviors

Freeze-dried hydrogels with confirmed weights (W_d) were immersed in different buffer solutions at pH 7.4, 4.0 and 1.2. At selected time intervals, the hydrated gels were carefully taken out and weighed (W_t) after the excess superficial buffer was removed with a wet filter paper. This procedure was repeated until no further weight increment occurred (W_e). The swelling ratio (SR) and equilibrium swelling ratio (ESR) were obtained according to the following expression:

$$SR = (W_t - W_d)/W_d \quad (1)$$

$$ESR = (W_e - W_d)/W_d \quad (2)$$

where, W_d represents the dry weight of the gel specimen, W_t represents the swollen weight of the gel specimen after a certain time and W_e represents the equilibrium swollen weight of the gel specimen. The swelling ratios in different concentration of KCl solution were tested in the same way.

The water retention (WR) in hydrogels during the deswelling step at 40 °C was evaluated gravimetrically in deionized water at pH 7.4, by eqn (3):

$$WR\ (\%) = (W_t - W_d)/(W_e - W_d) \times 100 \quad (3)$$

2.9. Drug loading and release

In this work, 5-fluorouracil was chosen as a model drug to explore the drug loading and release property of Salecan-*g*-PDMC. 5-Fluorouracil was incorporated into the Salecan-*g*-PDMC hydrogels by a swelling–diffusion approach. Briefly, powder of 5-fluorouracil was solubilized in a 0.01 M pH 9.18 phosphate buffers to gain the 5-fluorouracil solution (500 μg mL^{-1}). Subsequently, the lyophilized hydrogel sample of known weight (100 mg) was soaked in 20 mL of the 5-fluorouracil solution under shaking for 24 h. After drug solution (absorption) equilibrium was attained, all hydrogel samples were removed from the drug solution and washed with phosphate buffer three times to get rid of the surface adsorption of drug. The remnant 5-fluorouracil solution and the phosphate buffer used to rinse the 5-fluorouracil-loaded hydrogel samples were collected together. The content of 5-fluorouracil left in the loading solution was calculated utilizing the Bradford assay kit by UV-vis spectrophotometer (TU-1900, China) measurements at 268 nm.[6] The drug loading efficiency (DLE) was gained according to the equation below:

$$DLE\ (wt, \%) = (W_0 - W_e)/W_0 \times 100 \quad (4)$$

here, W_0 and W_e are the total mass of the 5-fluorouracil in immersing medium before and after loading of the hydrogel sample, respectively.

With regard to *in vitro* 5-fluorouracil release test, the above-mentioned 5-fluorouracil-loaded hydrogel samples were first soaked in 20 mL of buffer solutions (pH = 7.4 and 1.2) at 37 °C with shaking speed of 100 rpm. At selected time periods, 2 mL supernatant was withdrawn and replaced with 2 mL fresh buffer. The concentration of released 5-fluorouracil was quantified by UV-vis spectrophotometry at a wavelength of 268 nm and the cumulative percent 5-fluorouracil release was acquired by formula (5):

$$\text{Cumulative drug release } (\%) = \frac{2.0\sum C_{n-1} + 20C_n}{m} \times 100 \quad (5)$$

where, m represents the amount of 5-fluorouracil in the hydrogel sample before release, C_{n-1} is the concentration of 5-fluorouracil in the releasing media after $n-1$ withdrawing steps, and C_n denotes the concentration of 5-fluorouracil in the n^{th} hydrogel sample.

2.10. Cellular assays

2.10.1. Cell culture. African green monkey kidney cells (COS-7) and human embryonic kidney (HEK) 293T cells were acquired from Center for Molecular Metabolism (NJUST, China). Both of the cells were maintained in Dulbecco's modified Eagle medium (DMEM) containing 10% fetal bovine serum and 1% antibiotics (0.1 mg mL^{-1} streptomycin and 100 U mL^{-1} penicillin) in an incubator at 5% CO_2 and 37 °C. The culture medium was replaced every other day.

2.10.2. Cell compatibility. Cell compatibility of the designed hydrogels against two cell lines (COS-7 and HEK 293T cells) was analyzed using the 3-[4,5-dimethylthiazol-2-yl]-2,5-diphenyltetrazolium bromide (MTT) assay by an indirect extraction test according to ISO 10993-5 protocol.[32] Briefly, all gels were sterilized with ethanol (70%) followed by rinsing with sterile PBS (pH 7.4). Subsequently, the sterile gels were soaked in 20 mL of DMEM at 37 °C for 48 h. Next, the gels were carefully taken out from the DMEM medium and the acquired extract liquids were filtered through syringe filters (with pore size of 0.22 μm). At the same time, all cells were separately seeded into a 96-well plate (5000 cells per well) and maintained overnight to allow cell attachment. After that, the cell culture solution in each well was aspirated and changed with 200 μL of the hydrogel extracts. 24 h later, the culture medium was replaced with fresh DMEM containing 50 μL of MTT, and these two cells were cultured for another 4 h. Finally, the medium in each well was completed aspirated and the purple formazan crystal generated by viable cells was solubilized with 150 μL of dimethyl sulfoxide. The cell viability was computed by comparing the absorbance at 570 nm with control wells containing only cell culture media.

2.10.3. Cell adhesion. Sterilized hydrogel films (SGD4) were transferred into 6-well cell-culture plates with DMEM and cultured at 37 °C for 2 days. HEK 293T and COS-7 cells were seeded at a density of 1×10^4 cells per cm^2 on the surface of the gels and cultured in a 5% CO_2 atmosphere at 37 °C for 2 days, respectively. During the whole incubation period, the medium was refreshed every day. Finally, the cells were stained with ethidium bromide/acridine orange (EB/AO), and cell morphology was inspected through a phase-contrast optical microscope (OLYMPUS ckx31, Japan).

3 Results and discussions

3.1. Fabrication of Salecan-*g*-PDMC hydrogels

In this study, homogenous graft polymerization of the DMC onto the Salecan backbone was carried out utilizing MBAA as cross-linker and APS as radical initiator. The possible mechanism is outlined in Fig. 1. First, the initiator APS was decomposed by heating to produce sulfate anion-radicals. Second, these anion radicals extracted hydrogen from the –OH groups of the active ingredients in Salecan skeleton to generate macro-radicals, leading to active centers on the polysaccharide backbone.[14] Third, the monomer molecules (DMC), close to these active sites, turn into acceptors of macro-radicals, causing chain initiation and afterward themselves converted into free radical donors, which resulted in the growth of graft chain. Finally, in the chain propagation period, the end vinyl groups of the MBAA cross-linker reacted with the as-formed polymer chains, thereby, the copolymer hydrogel composed of a cross-linked architecture was formed.[19,33]

3.2. FT-IR

FT-IR spectroscopy was employed to obtain structural information of Salecan, Salecan-*g*-PDMC (SGD4) and pure PDMC hydrogels as clearly depicted in Fig. 2(a). In case of Salecan, a broad absorption peak located at approximately 3290 cm^{-1} belonged to the O–H stretching vibration.[18] Characteristic bands of Salecan emerged in the region of 1100–800 cm^{-1}.[16,18] More specifically, the peak entered at 1040 cm^{-1} was ascribed to C–OH stretching of glucopyranose, a weak band at 896 cm^{-1} displayed that D-glucopyranose possessed β-configuration and a small absorption peak emerged in 813 cm^{-1} was associated with the existence of a little α-glucopyranose.[14,32] With regard to the FT-IR curve of PDMC, the characteristic peak at 1723 cm^{-1} was due to the stretching vibrations of the carbonyl group, and the bands at 1477 and 951 cm^{-1} were attributed to the bending and stretching vibrations of quaternary ammonium group, respectively.[34] The spectrum of Salecan-*g*-PDMC hydrogel displays a mixture of PDMC and Salecan signals, similar to pure PDMC but with some discrimination. For example, the PDMC segment was verified by the appearance of feature peaks of quaternary ammonium groups at 1476 and 948 cm^{-1} (bending and stretching vibrations),[34] whereas the presence of peak at 893 cm^{-1} was characteristic of the Salecan chains.[26] Particularly, the typical absorption peak of Salecan at 893 cm^{-1} was obviously weakened after the graft reaction, demonstrating the participation of Salecan in the copolymerization reaction. Following the literature, similar results were acquired for other polysaccharide-based graft copolymers.[15,35] These observations indicated that the PDMC chains were successfully grafted onto the Salecan backbone.

3.3. XRD studies

XRD patterns of the Salecan powders, PDMC and Salecan-*g*-PDMC (SGD4) hydrogels are depicted in Fig. 2(b). The diffraction spectra of Salecan demonstrated a single peak centred at around $2\theta = 21°$, which can be ascribed to the crystalline regions of the Salecan structure. These crystalline regions are established by the hydrogen bonds among –OH groups of Salecan.[14] Similar results were acquired for other polysaccharides, such as cellulose[36] and chitosan.[37] Nevertheless, for the XRD curve of Salecan-*g*-PDMC hydrogel, the characteristic peak intensity of Salecan reduced drastically. The reason was that the grafting of DMC onto Salecan chain occurred in a random manner along Salecan backbone, resulting in the destruction of those formed crystalline regions of Salecan.[14]

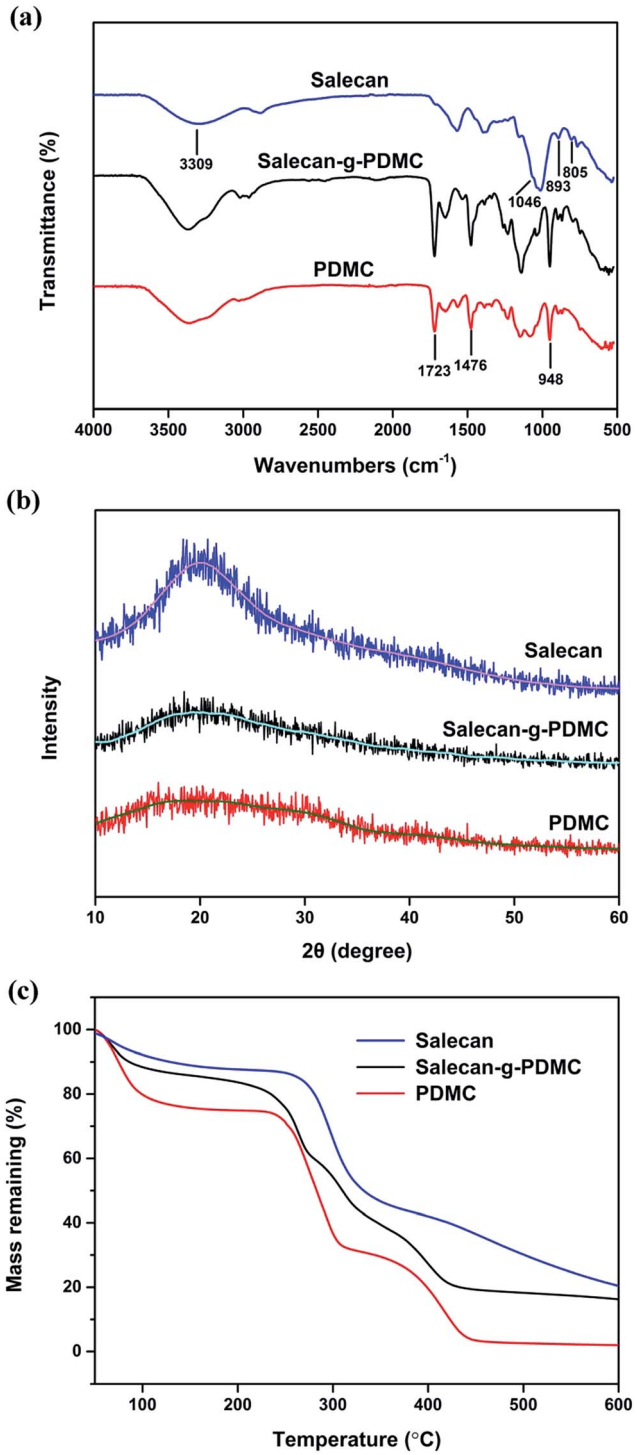

Fig. 2 FT-IR spectra (a), XRD patterns (b) and TGA thermograms (c) of Salecan, PDMC and Salecan-*g*-PDMC (SGD4) hydrogels.

3.4. TGA

The thermal stability of the Salecan, pristine PDMC and Salecan-*g*-PDMC (SGD4) hydrogels was evaluated by TGA technique (Fig. 2(c)). For Salecan, an initial 11.9% of mass loss taken placed in the 50–205 °C temperature range, indicating the expulsion of moisture absorbed from the air. Subsequently, approximately 44.7% mass loss occurred in the range of 205–370 °C, and further a 25.1% mass loss appeared between 370 and 600 °C, which was attributed to the splitting of Salecan main chain.[14] In the case of the pure PDMC thermogram, a three-stage degradation process was noticed. The first stage (50–220 °C, 25.3% weight loss) was because of the evaporation of residual water; the second stage (220–312 °C, 42.2% weight loss) involved the degradation of ammonium quaternary groups; the third stage (312–600 °C, 28.8% weight loss) was due to the destruction of the residual chain.[38]

As can be seen from the Fig. 2(c), Salecan was more stable than PDMC gel sample. The glycosidic bonds that join Salecan polysaccharides appear to be more stable than the chemical-covalent bonds that join the hydrogels. The grafted copolymer hydrogel underwent four steps of weight loss. The previous slight weight loss (nearly 17.1%) below 210 °C was assigned to desorption of bound water. The second and third steps were located at 210–271 °C (20.3% weight loss) and 271–328 °C (19.0% weight loss). The fourth step started from 328 °C, and 26.9% decomposition was observed at 600 °C. The latter three steps corresponded to a complex process where scission of the PDMC chain, breakage of the gel network and fragmentation of the Salecan skeleton was dominant.[27]

3.5. Rheological behaviors

As hydrogel drug carriers, their most important features are their mechanical strength and elasticity.[16] The rheological study can disclose the quantity of energy stored in the gel system (storage modulus, G') and energy dissipated within the gel system (loss modulus, G'').[39] Hence, investigation of the rheological properties of the resulting hydrogels was carried out (Fig. 3(a) and (b)). The solid-like features of these produced gels were distinctly verified by the fact that storage modulus and loss modulus were both nearly independent of frequency over the range of frequencies measured in this study, and further confirmed as the G' value was bigger than that of G'' at all frequencies tested.[40] Furthermore, it can be observed from Fig. 3(a) that the mechanical strength of formed hydrogel was easily controlled by altering the concentration of Salecan utilized to prepare the hydrogel. Specifically, before the graft reaction, the pristine PDMC hydrogel owned the strongest G' value of about 1171 Pa. By elevating the content of Salecan in the pregel solution to 2.5, 5, 7.5 and 10 mL, the G' value gradually decreased to nearly 824, 600, 295 and 132 Pa, respectively. One explanation was that the incorporation of Salecan content in the hydrogel composition helped bring a higher swelling value (as will be described below), which caused a reduction in gel stiffness.

3.6. Swelling experiment

One particular characteristic of fabricated hydrogels is their capacity to uptake and retain water without losing their structure integrity.[41] The levels of responsiveness, swelling and deswelling are important features to take into consideration when designing hydrogels for drug carriers. Therefore, the swelling property of the Salecan-*g*-PDMC hydrogels was comprehensively assessed.

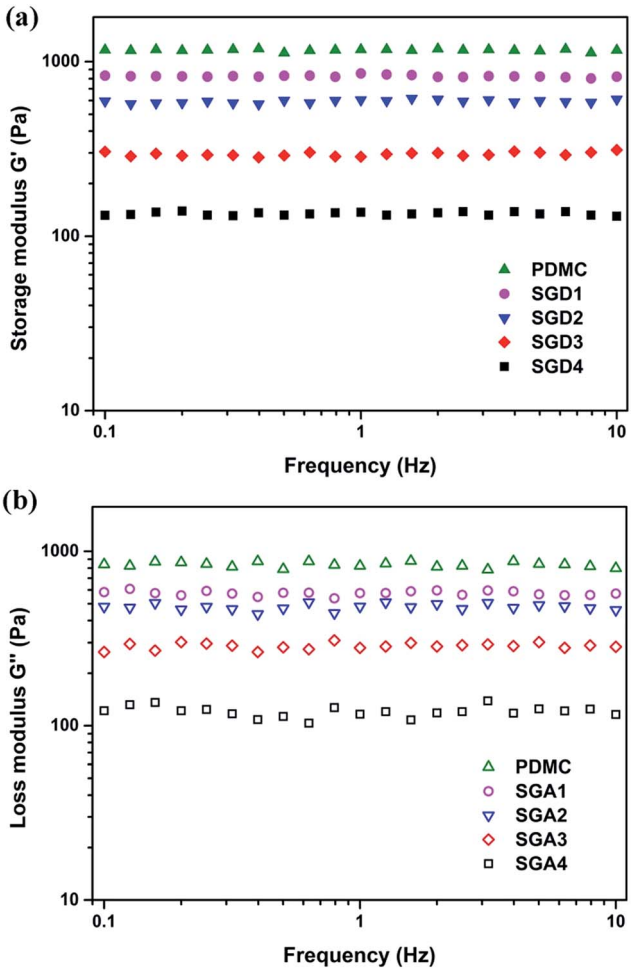

Fig. 3 Frequency dependence of (a) storage modulus and (b) loss modulus of PDMC and Salecan-*g*-PDMC hydrogels.

3.6.1. Swelling kinetics of grafted hydrogels. The dynamic swelling features of the resulting hydrogels in pH 4.0 buffers were measured to understand the effect of Salecan dose on the water uptake behaviors (Fig. 4(a)). All hydrogel samples rapidly hydrated in the first four hours and approached to equilibrium after ten hours; as the Salecan contents increased, the equilibrium swelling ratio (ESR) raised. Taking SGD1 for example, a rapid swelling was observed at the initial stage of swelling (from 0 to 4 h), and achieved saturation with an ESR of 32.4 after 10 h. As for the other three investigated groups (SGD2, SGD3 and SGD4) with distinct incorporation ratios of Salecan, the capability to absorb water was increased remarkably (42.6 for SGD2, 58.7 for SGD3 and 66.3 for SGD4). An explanation for this phenomenon was ascribed to the existence of a high density of hydroxyl groups on the Salecan chains that attract water from the incubation media, benefiting to the diffusion of water into gel matrix, and eventually, increasing water uptake ability.[16,26] Overall, dynamic swelling experiment showed that the swelling properties of the as-prepared grafted hydrogels were found to be tunable by regulating the hydrophilicity of the gel sample, which can easily be controlled by adjusting the Salecan amount.

3.6.2. Influence of pH on water uptake. To evaluate the influence of pH on water absorption, the equipment swelling ratio (ESR) was recorded for designed gels in buffer solutions of pH 7.4, 4.0 and 1.2, respectively. As presented in Fig. 4(b), the overall feeling was that all of the tested hydrogels exhibited a similar trend with distinct extent of water uptake, namely, the ESR decreased consecutively from pH 1.2 to 7.4. For example, the ESR values of SGD4 were 86.1 for pH 1.2, 66.3 for pH 4.0 and 49.4 for pH 7.4. The designed semi-IPN hydrogel was pH-sensitive due to the contribution of ionic group $-N^{+}(CH_3)_3$. When the pH of the solution was increased, the degree of ionization of semi-IPN gels reduced.[42] This would result in that the electrostatic repulsion between the chains of semi-IPN hydrogels decreased, restricting water absorption. In sum, equilibrium swelling studies clearly revealed that the developed hydrogels were able to respond to environmental pH, making them quite attractive to serve as pH-responsive drug delivery vehicles.

3.6.3. Effect of ionic strength on swelling. To assess the effect of ion concentration on the swelling behavior of Salecan-*g*-PDMC gel samples, the values of ESR as a function of potassium chloride concentration are plotted in Fig. 4(c). As displayed in Fig. 4(c), there was the same decreasing tendency for the equilibrium water absorption of the hydrogel in KCl solution with the addition of saline solution dose. Regardless of hydrogel types, the ESR value dropped distinctly as the KCl concentration raised. Specifically, the ESR values of SGD3 were 36.6, 25.3 and 15.4 for KCl concentration (%, w/w) = 0.4, 0.8 and 1.2, respectively. The mechanisms of these results can be understood as follows. On the one hand, the salt ions penetrated into the gel network and combined with ionized groups of PDMC chains, leading to the shielding effect and weakening the electrostatic repulsion. Therefore, the water molecules were easily squeezed out.[14,42] On the other hand, the osmotic pressure between interior hydrogel and external swelling solution was reinforced when the KCl concentration enhanced. In this case, water in the inside architecture of the hydrogel tended to diffuse out to the culture medium, causing reduction of water uptake ability.[9,18]

3.6.4. Water retention test. Fig. 4(d) presents the deswelling profile of grafted hydrogels at 40 °C as a function of time. As observed from Fig. 4(d), the Salecan-*g*-PDMC hydrogels containing more Salecan lost water at a faster rate and released more water within the identical time intervals. For example, SGD1 released over 88.4% of its absorbed water after 500 min whereas, during the equal time intervals, the SGD2, SGD3 and SGD4, lost about 92.8%, 95.7% and 97.1% of their water, respectively. Addition of the hydrophilic polysaccharide (Salecan), which can act as water-releasing channels, promoted the removal of water when hydrogel network crumbled.[43]

3.7. Morphology of the Salecan-*g*-PDMC hydrogels

The microstructure of the hydrogel directly influences its later application as a drug carrier, while the drug adsorption and release properties will be affected by the pore size and surface area of the hydrogel.[16] Hence, we inspected the morphology of

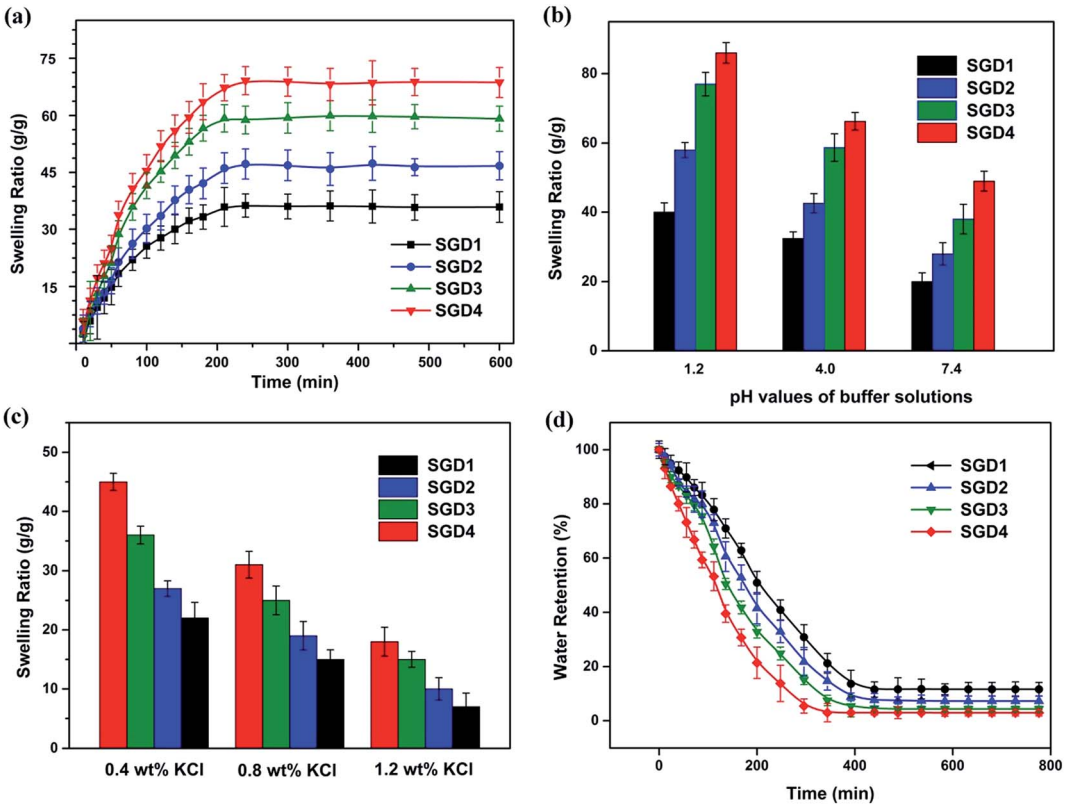

Fig. 4 Swelling behavior of the Salecan-*g*-PDMC hydrogels: swelling kinetic in deionized water (a), equilibrium swelling values in different buffer solutions (b) and KCl solutions (c); water retention (d).

the designed hydrogels. Cryo-SEM was employed here to confirm that the morphology of each hydrogel was well-retained. As presented in Fig. 5, all hydrogel formulations revealed ordered and uniform porous networks, resembling other freeze-dried hydrogel.[9,44] We also observed that the gel with higher Salecan content possessed larger pores, compared with that of lower Salecan concentration. For instance, SGD1 had the smallest pore size with a diameter of 38.3 ± 10.5 μm among the four samples, while the average pore diameter enhanced to approximately 53.4 ± 11.6 μm, 84.7 ± 24.8 μm and 102.4 ± 25.7 μm for SGD2, SGD3 and SGD4, respectively. An explanation was that the addition of Salecan enhanced the water uptake capacity of the hydrogel, which in turn expanded the space for water reservation. In this case, water molecules were easy to penetrate into the hydrogel matrices, being prone to the formation of greater ice crystal during lyophilized process. Therefore, larger pores were yielded after water sublimation.[14,45]

3.8. *In vitro* drug loading and release

3.8.1. 5-Fluorouracil loading efficiency. Here, 5-fluorouracil, a widely used drug in cancer treatment, was chosen as a model drug and introduced into the polymeric network by a swelling–diffusion approach.[10,46] Fig. 6(a) displays the drug loading efficiency (DLE) of the grafted hydrogel. As can be seen from Fig. 6(a), the 5-fluorouracil loading efficiency enhanced with the increase of Salecan dose. For instance, SGD4 containing 8 mL of Salecan showed the highest 5-fluorouracil loading efficiency of 66.3% while the SGD1 with 2 mL of Salecan only exhibited a smallest 5-fluorouracil loading efficiency of 32.4%. Interesting, the trend of drug loading efficiency was the same as that of water uptake values for these hydrogels discussed above. Because of the identical concentration of 5-fluorouracil solution for drug loading, gel with stronger hydration ability could

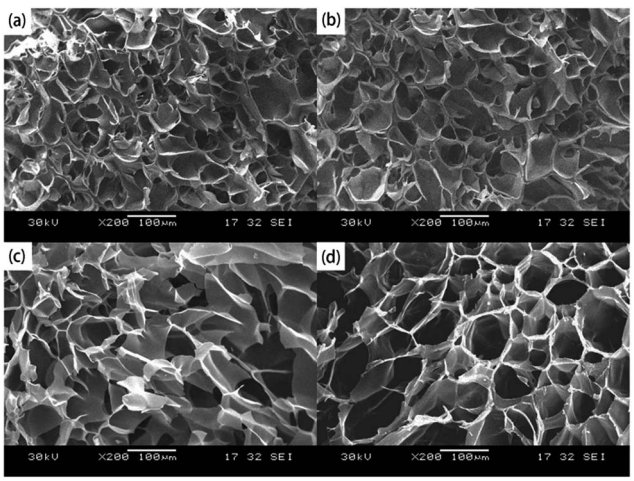

Fig. 5 SEM graphs of the grafted hydrogels: (a) SGD1, (b) SGD2, (c) SGD3 and (d) SGD4. Scale bars represent 100 μm.

uptake more 5-fluorouracil solution. Ultimately, the amount of 5-fluorouracil loading increased with the improvement of Salecan dose used in the pre-gel solution.[9,26]

3.8.2. Drug release. To identify the release behaviors of 5-fluorouracil from the Salecan-*g*-PDMC hydrogels, *in vitro* release studies were conducted in buffer solutions with pH values of 7.4 and 1.2 at 37 °C (simulating the pH conditions of colon and stomach in the body). It can be seen from Fig. 6(b) and (c) that the amount of 5-fluorouracil escaped from 5-fluorouracil-loaded samples was pH-dependent. When pH of the release medium was reduced from 7.4 to 1.2, 5-fluorouracil release was greatly increased. Specifically, after 21 h, the cumulative release in pH 7.4 buffers was 23.1%, 29.6%, 33.7% and 38.0% for SGD1, SGD2, SGD3 and SGD4, respectively, but such value increased to 54.3%, 62.2%, 71.0% and 78.8% for the corresponding hydrogel in the pH 1.2 media. These differences in release can be explained by the next two factors. (1) At pH 1.2 (The isoelectric point of 5-fluorouracil is 8.0,[47] so the 5-fluorouracil carries a positive charge at the normal physiological environment.), the strong electrostatic repulsion between $-N^{+}(CH_3)_3$ and positively charged drug facilitated the release of 5-fluorouracil.[42] (2) When the pH of the release media was increased to 7.4, the solubility of 5-fluorouracil was decreased, restricting the liberation of 5-fluorouracil.[6]

Apart from the influences of different pHs, it is also noticed in Fig. 6(b) and (c) that the drug release was Salecan-dose dependent, *i.e.*, after 21 h, the amount of 5-fluorouracil released from the graft hydrogels was in the order of SGD4 > SGD3 > SGD2 > SGD1. This phenomenon could be illustrated by considering the formation of denser structures when gels possessed lower Salecan content, which hindered the escape of entrapped 5-fluorouracil from the gel matrix.[10,17] Collectively, the 5-fluorouracil release from the hydrogel could be adjusted by simply modulating the pH value of the release medium and Salecan amount in the gel compositions.

3.9. Cell compatibility of the grafted hydrogel samples

Cytotoxicity is a significant factor when selecting appropriate vectors for drug delivery.[48] To act as safe drug carrier, the device itself was required to have a low toxicity. Here, the cytotoxicities of the Salecan-*g*-PDMC hydrogels were assessed in HEK 293T and COS-7 cells utilizing an indirect MTT assay. First, these two cells were cultured with different extracts of Salecan-*g*-PDMC hydrogel samples for 24 h. As evidenced in Fig. 6(d), after 24 h incubation, all experiment groups displayed nearly no cytotoxicity toward HEK 293T and COS-7 cells (cell viability > 90%), indicating the good biocompatibility of these designed Salecan-based drug delivery vehicles.[14]

To further illustrate the low cytotoxicity of Salecan-*g*-PDMC hydrogels, a live/dead assay was also conducted for visualization of cell viability by inverted microscope. The representative micrographs of HEK 293T and COS-7 cells incubated with the tissue culture polystyrene dishes (TCPS) and grafted hydrogel are presented in Fig. 7. EB-stained dead cells are in red and AO

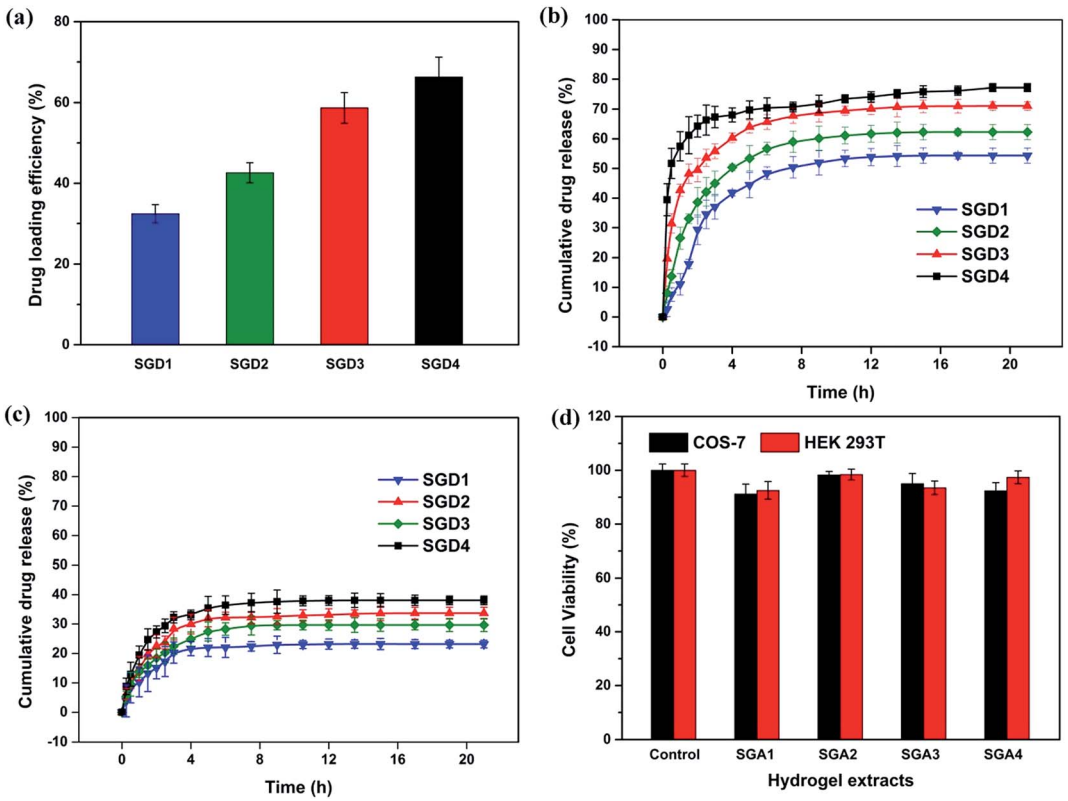

Fig. 6 (a) Loading efficiency of the hydrogel samples. *In vitro* 5-fluorouracil release curves from the hydrogels at pH 1.2 (b) and pH 7.4 (c). (d) Cell viability of HEK 293T cells and COS-7 cells after treatment with hydrogel extracts.

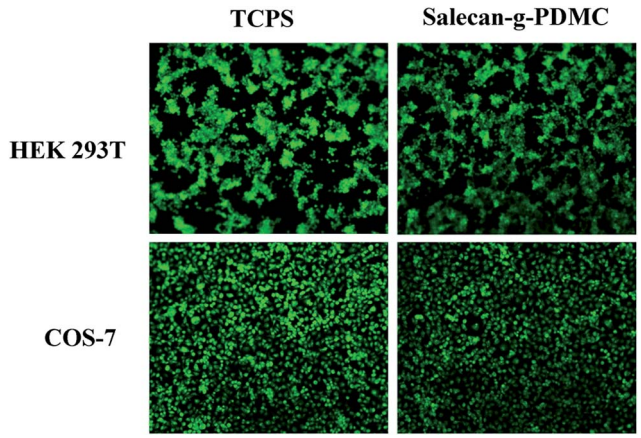

Fig. 7 Phase-contrast micrographs (100×) of fluorescence images of HEK 293T cells and COS-7 cells cultured on tissue culture polystyrene dishes (TCPS) and Salecan-*g*-PDMC hydrogel surface after 2 days.

stained living cells are in green.[49] Obviously, a large number of green fluorescence and hardly any red fluorescence can be observed for Salecan-based gels similar to that seen on negative control. These results also suggested the biocompatibility of the Salecan-based drug delivery device itself, which was consistent with the data obtained in MTT assay.

4 Conclusions

A new Salecan-based hydrogel drug devices was fabricated by grafting [2-(methacryloxy)ethyl]trimethylammonium chloride onto Salecan chains in the presence of cross-linker MBAA using APS as an initiator. By varying the concentration of Salecan in the precursor solution, the water content, mechanical strength, pore size and 5-fluorouracil loading/release of the hydrogels can be readily modulated. Moreover, the designed Salecan-based hydrogel was cell compatible and supported the cell proliferation. With these excellent features, our hydrogel may serve as a versatile and facile platform for oral drug delivery applications.

Acknowledgements

The work is supported by the National Natural Science Foundation of China (51573078) and Fundamental Research Funds for the Central Universities (30920130121013).

References

1 K. Ganguly, K. Chaturvedi, U. A. More, M. N. Nadagouda and T. M. Aminabhavi, Polysaccharide-based micro/nanohydrogels for delivering macromolecular therapeutics, *J. Controlled Release*, 2014, **193**, 162–173.

2 E. S. Dragan, D. F. Apopei Loghin, A.-I. Cocarta and M. Doroftei, Multi-stimuli-responsive semi-IPN cryogels with native and anionic potato starch entrapped in poly(*N*,*N*-dimethylaminoethyl methacrylate) matrix and their potential in drug delivery, *React. Funct. Polym.*, 2016, **105**, 66–77.

3 T. M. Aminabhavi, M. N. Nadagouda, U. A. More, S. D. Joshi, V. H. Kulkarni, M. N. Noolvi and P. V. Kulkarni, Controlled release of therapeutics using interpenetrating polymeric networks, *Expert Opin. Drug Delivery*, 2015, **12**, 669–688.

4 J. Y. Lai and A. C. Hsieh, A gelatin-*g*-poly(*N*-isopropylacrylamide) biodegradable *in situ* gelling delivery system for the intracameral administration of pilocarpine, *Biomaterials*, 2012, **33**(7), 2372–2387.

5 G. E. Giammanco, C. T. Sosnofsky and A. D. Ostrowski, Light-responsive iron(III)-polysaccharide coordination hydrogels for controlled delivery, *ACS Appl. Mater. Interfaces*, 2015, **7**(5), 3068–3076.

6 I. M. El-Sherbiny, R. J. Lins, E. M. Abdel-Bary and D. R. K. Harding, Preparation, characterization, swelling and *in vitro* drug release behaviour of poly[*N*-acryloylglycine-chitosan] interpolymeric pH and thermally-responsive hydrogels, *Eur. Polym. J.*, 2005, **41**(11), 2584–2591.

7 N. Paradee and A. Sirivat, Electrically controlled release of benzoic acid from poly(3,4-ethylenedioxythiophene)/alginate matrix: effect of conductive poly(3,4-ethylenedioxythiophene) morphology, *J. Phys. Chem. B*, 2014, **118**(31), 9263–9271.

8 J. Li, L. Ma, G. Chen, Z. Zhou and Q. Li, A high water-content and high elastic dual-responsive polyurethane hydrogel for drug delivery, *J. Mater. Chem. B*, 2015, **3**(42), 8401–8409.

9 E. S. Dragan and A. I. Cocarta, Smart Macroporous IPN Hydrogels Responsive to pH, Temperature, and Ionic Strength: Synthesis, Characterization, and Evaluation of Controlled Release of Drugs, *ACS Appl. Mater. Interfaces*, 2016, **8**(19), 12018–12030.

10 X. Gao, Y. Cao, X. Song, Z. Zhang, C. Xiao, C. He and X. Chen, pH- and thermo-responsive poly(*N*-isopropylacrylamide-*co*-acrylic acid derivative) copolymers and hydrogels with LCST dependent on pH and alkyl side groups, *J. Mater. Chem. B*, 2013, **1**(41), 5578–5587.

11 O. Cevik, D. Gidon and S. Kizilel, Visible-light-induced synthesis of pH-responsive composite hydrogels for controlled delivery of the anticonvulsant drug pregabalin, *Acta Biomater.*, 2015, **11**, 151–161.

12 H. J. Sim, T. Thambi and D. S. Lee, Heparin-based temperature-sensitive injectable hydrogels for protein delivery, *J. Mater. Chem. B*, 2015, **3**(45), 8892–8901.

13 Y. Nakagawa, S. Nakasako, S. Ohta and T. Ito, A biocompatible calcium salt of hyaluronic acid grafted with polyacrylic acid, *Carbohydr. Polym.*, 2015, **117**, 43–53.

14 X. Hu, W. Wei, X. Qi, H. Yu, L. Feng, J. Li, S. Wang, J. Zhang and W. Dong, Preparation and characterization of a novel pH-sensitive Salecan-*g*-poly(acrylic acid) hydrogel for controlled release of doxorubicin, *J. Mater. Chem. B*, 2015, **3**(13), 2685–2697.

15 X. F. Sun, H. H. Wang, Z. X. Jing and R. Mohanathas, Hemicellulose-based pH-sensitive and biodegradable hydrogel for controlled drug delivery, *Carbohydr. Polym.*, 2013, **92**(2), 1357–1366.

16 X. Qi, W. Wei, J. Li, G. Zuo, X. Hu, J. Zhang and W. Dong, Development of novel hydrogels based on Salecan and poly(*N*-isopropylacrylamide-*co*-methacrylic acid) for

controlled doxorubicin release, *RSC Adv.*, 2016, **6**(74), 69869–69881.

17 Y. Bai, Z. Zhang, A. Zhang, L. Chen, C. He, X. Zhuang and X. Chen, Novel thermo- and pH-responsive hydroxypropyl cellulose- and poly(L-glutamic acid)-based microgels for oral 5-fluorouracil controlled release, *Carbohydr. Polym.*, 2012, **89**(4), 1207–1214.

18 X. Qi, W. Wei, J. Li, Y. Liu, X. Hu, J. Zhang, L. Bi and W. Dong, Fabrication and Characterization of a Novel Anticancer Drug Delivery System: Salecan/Poly(methacrylic acid) Semi-interpenetrating Polymer Network Hydrogel, *ACS Biomater. Sci. Eng.*, 2015, **1**(12), 1287–1299.

19 X. W. Peng, J. L. Ren, L. X. Zhong, F. Peng and R. C. Sun, Xylan-rich hemicelluloses-*graft*-acrylic acid ionic hydrogels with rapid responses to pH, salt, and organic solvents, *J. Agric. Food Chem.*, 2011, **59**(15), 8208–8215.

20 X. Tian, E. Ren, J. Wang, J. Zou, Y. Tao, S. Wang and X. Jiang, Synthesis and flocculation property in dye solutions of β-cyclodextrin–acrylic acid–[2-(acryloyloxy)ethyl]trimethyl ammonium chloride copolymer, *Carbohydr. Polym.*, 2012, **87**(3), 1956–1962.

21 A. Xiu, Y. Kong, M. Zhou, B. Zhu, S. Wang and J. Zhang, The chemical and digestive properties of a soluble glucan from *Agrobacterium* sp. ZX09, *Carbohydr. Polym.*, 2010, **82**(3), 623–628.

22 L. Xu and J. Zhang, Bacterial glucans: production, properties, and applications, *Appl. Microbiol. Biotechnol.*, 2016, **100**(21), 9023–9036.

23 A. Xiu, Y. Zhan, M. Zhou, B. Zhu, S. Wang, A. Jia, W. Dong, C. Cai and J. Zhang, Results of a 90-day safety assessment study in mice fed a glucan produced by *Agrobacterium* sp. ZX09, *Food Chem. Toxicol.*, 2011, **49**(9), 2377–2384.

24 A. Xiu, M. Zhou, B. Zhu, S. Wang and J. Zhang, Rheological properties of Salecan as a new source of thickening agent, *Food Hydrocolloids*, 2011, **25**(7), 1719–1725.

25 X. Qi, J. Li, W. Wei, T. Su, G. Zuo, X. Pan, J. Zhang and W. Dong, Preparation of a Salecan/poly(2-acrylamido-2-methylpropanosulfonic acid-*co*-[2-(methacryloxy)ethyl] trimethylammonium chloride) semi-IPN hydrogel for drug delivery, *ChemMedChem*, 2017, **12**, 120–129.

26 W. Wei, X. Qi, J. Li, G. Zuo, W. Sheng, J. Zhang and W. Dong, Smart Macroporous Salecan/Poly(*N*,*N*-diethylacrylamide) Semi-IPN Hydrogel for Anti-Inflammatory Drug Delivery, *ACS Biomater. Sci. Eng.*, 2016, **2**(8), 1386–1394.

27 X. Qi, W. Wei, J. Li, G. Zuo, X. Pan, T. Su, J. Zhang and W. Dong, Salecan-Based pH-Sensitive Hydrogels for Insulin Delivery, *Mol. Pharmaceutics*, 2017, **14**, 431–440.

28 P. V. Dadhaniya, M. P. Patel and R. G. Patel, Removal of anionic dyes from aqueous solution using poly[*N*-vinyl pyrrolidone/2-(methacryloyloxyethyl) trimethyl ammonium chloride] superswelling hydrogels, *Polym. Bull.*, 2006, **58**(2), 359–369.

29 B. L. Rivas, H. A. Maturana, I. M. Perič and S. Villegas, Metal ion extraction behavior of poly([2 (methacryloyloxy)ethyl] trimethylammonium chloride-*co*-acrylic acid) resin, *Polym. Bull.*, 1999, **43**(2–3), 277–283.

30 R. K. Mishra, K. Ramasamy, N. A. Ahmad, Z. Eshak and A. B. Majeed, pH dependent poly[2-(methacryloyloxyethyl) trimetylammonium chloride-*co*-methacrylic acid] hydrogels for enhanced targeted delivery of 5-fluorouracil in colon cancer cells, *J. Mater. Sci.: Mater. Med.*, 2014, **25**(4), 999–1012.

31 A. La Gatta, C. Schiraldi, A. Esposito, A. D'Agostino and A. De Rosa, Novel poly(HEMA-*co*-METAC)/alginate semi-interpenetrating hydrogels for biomedical applications: synthesis and characterization, *J. Biomed. Mater. Res., Part A*, 2009, **90**(1), 292–302.

32 X. Qi, X. Hu, W. Wei, H. Yu, J. Li, J. Zhang and W. Dong, Investigation of Salecan/poly(vinyl alcohol) hydrogels prepared by freeze/thaw method, *Carbohydr. Polym.*, 2015, **118**, 60–69.

33 M. Zhang, Z. Cheng, T. Zhao, M. Liu, M. Hu and J. Li, Synthesis, characterization, and swelling behaviors of salt-sensitive maize bran-poly(acrylic acid) superabsorbent hydrogel, *J. Agric. Food Chem.*, 2014, **62**(35), 8867–8874.

34 N. B. Shukla, S. Rattan and G. Madras, Swelling and Dye-Adsorption Characteristics of an Amphoteric Superabsorbent Polymer, *Ind. Eng. Chem. Res.*, 2012, **51**(46), 14941–14948.

35 W. Wang and A. Wang, Synthesis and swelling properties of pH-sensitive semi-IPN superabsorbent hydrogels based on sodium alginate-*g*-poly(sodium acrylate) and polyvinylpyrrolidone, *Carbohydr. Polym.*, 2010, **80**(4), 1028–1036.

36 Y. Guo, X. Wang, X. Shu, Z. Shen and R. C. Sun, Self-assembly and paclitaxel loading capacity of cellulose-*graft*-poly(lactide) nanomicelles, *J. Agric. Food Chem.*, 2012, **60**(15), 3900–3908.

37 E. S. Costa-Júnior, E. F. Barbosa-Stancioli, A. A. P. Mansur, W. L. Vasconcelos and H. S. Mansur, Preparation and characterization of chitosan/poly(vinyl alcohol) chemically cross-linked blends for biomedical applications, *Carbohydr. Polym.*, 2009, **76**(3), 472–481.

38 N. K. Goel, M. S. Rao, V. Kumar, Y. K. Bhardwaj, C. V. Chaudhari, K. A. Dubey and S. Sabharwal, Synthesis of antibacterial cotton fabric by radiation-induced grafting of [2-(methacryloyloxy)ethyl]trimethylammonium chloride (MAETC) onto cotton, *Radiat. Phys. Chem.*, 2009, **78**(6), 399–406.

39 W. Zheng, L. J. Chen, G. Yang, B. Sun, X. Wang, B. Jiang, G. Q. Yin, L. Zhang, X. Li, M. Liu, G. Chen and H. B. Yang, Construction of Smart Supramolecular Polymeric Hydrogels Cross-linked by Discrete Organoplatinum(II) Metallacycles *via* Post-Assembly Polymerization, *J. Am. Chem. Soc.*, 2016, (14), 4927–4937.

40 B. Jiang, W. L. Hom, X. Chen, P. Yu, L. C. Pavelka, K. Kisslinger, J. B. Parise, S. R. Bhatia and R. B. Grubbs, Magnetic Hydrogels from Alkyne/Cobalt Carbonyl-Functionalized ABA Triblock Copolymers, *J. Am. Chem. Soc.*, 2016, **138**(13), 4616–4625.

41 A. Pascual, J. P. Tan, A. Yuen, J. M. Chan, D. J. Coady, D. Mecerreyes, J. L. Hedrick, Y. Y. Yang and H. Sardon, Broad-spectrum antimicrobial polycarbonate hydrogels

with fast degradability, *Biomacromolecules*, 2015, **16**(4), 1169–1178.

42 Y. Y. Hu, J. Zhang, Q. C. Fang, D. M. Jiang, C. C. Lin, Y. Zeng and J. S. Jiang, Salt and pH Sensitive Semi-Interpenetrating Polyelectrolyte Hydrogels Poly(HEMA-*co*-METAC)/PEG and Its BSA Adsorption Behavior, *J. Appl. Polym. Sci.*, 2015, **132**(9), 41537.

43 U. Haldar, M. Nandi, B. Maiti and P. De, POSS-induced enhancement of mechanical strength in RAFT-made thermoresponsive hydrogels, *Polym. Chem.*, 2015, **6**(28), 5077–5085.

44 J. Zhang, P. Du, D. Xu, Y. Li, W. Peng, G. Zhang, F. Zhang and X. Fan, Near-Infrared Responsive MoS2/Poly(*N*-isopropylacrylamide) Hydrogels for Remote Light-Controlled Microvalves, *Ind. Eng. Chem. Res.*, 2016, **55**(16), 4526–4531.

45 M. V. Dinu, M. Pradny, E. S. Dragan and J. Michalek, Ice-templated hydrogels based on chitosan with tailored porous morphology, *Carbohydr. Polym.*, 2013, **94**(1), 170–178.

46 Z. Liu and P. Yao, Versatile injectable supramolecular hydrogels containing drug loaded micelles for delivery of various drugs, *Polym. Chem.*, 2014, **5**(3), 1072.

47 E. Wenande, U. H. Olesen, M. M. Nielsen, C. Janfelt, S. H. Hansen, R. R. Anderson and M. Haedersdal, Fractional laser-assisted topical delivery leads to enhanced, accelerated and deeper cutaneous 5-fluorouracil uptake, *Expert Opin. Drug Delivery*, 2016, 1–11.

48 K. Chaturvedi, K. Ganguly, M. N. Nadagouda and T. M. Aminabhavi, Polymeric hydrogels for oral 5-fluorouracil delivery, *J. Controlled Release*, 2013, **165**, 129–138.

49 X. Li, Y. Wang, J. Chen, Y. Wang, J. Ma and G. Wu, Controlled release of protein from biodegradable multi-sensitive injectable poly(ether-urethane) hydrogel, *ACS Appl. Mater. Interfaces*, 2014, **6**(5), 3640–3647.